can speculatively be associated with the various known $\pi-p$ phenomena. The conjectured total angular momenta are stated in parentheses; the values given are those possibly inferred from simple Regge-pole-trajectory behavior. The two peaks discovered by Diddens *et al.*,[23] at pion energies of 1950 MeV for $\pi^- - p$, and 2370 MeV for $\pi^+ - p$, are included in the table upon

this basis of conjecture. The resonance points on a Regge plot are shown in Fig. 10, which illustrates the basis for the values given in parentheses in Table III. Diddens *et al.*[23] have discussed other assignments also to be considered for the two highest energy resonances.

ACKNOWLEDGMENT

The authors would like to acknowledge the assistance by the same persons as in the preceding article.[1]

[23] A. N. Diddens, E. W. Jenkins, T. F. Kycia, and K. F. Riley, Phys. Rev. Letters **10**, 262 (1963).

On the Analytic Structure of Production Amplitudes*

RUDOLPH C. HWA

Lawrence Radiation Laboratory, University of California, Berkeley, California

(Received 20 January 1964)

The analytic structure of two-particle to three-particle production amplitudes is examined within the framework of analytic S-matrix theory, with particular emphasis on the structure of the physical sheet. The basic principle used is maximal analyticity, which is both discussed and exemplified. The knowledge of the structure of the physical sheet is used in deriving formulas for the discontinuities across the cuts in the two-particle subenergies of the three-particle channel and across the cut in the total energy.

I. INTRODUCTION

THE determination of the precise content of the principle of maximal analyticity is an important problem in analytic S-matrix theory.[1] This principle asserts that scattering amplitudes, regarded as analytic functions of appropriate variables, have only the singularities required by general properties of the amplitudes.[2] Associated with the problem of determining the locations of these singularities are many questions regarding the sheet structure of the Riemann surface and the discontinuities across branch cuts. It remains to be shown on the basis of maximal analyticity that one can construct a single "physical" sheet, which contains all the physical points. Moreover, even with the assurance of the existence of the physical sheet, there are still questions regarding the structure of the singularities on that sheet and how one analytically continues from one physical region to another. Though the situation is relatively simple for scattering processes involving two particles only, it is not at all well understood when channels containing three or more particles are taken into consideration. Complications arise not only because of the increase in the number of variables necessary to describe the processes, but also because of the possibility of overlapping normal cuts

and the inevitable emergence of complex and anomalous cuts. In this paper we shall examine for the case of a production amplitude some of the simple ways in which these problems arise, and how they may be resolved.

Our ultimate aim here is to derive the discontinuities across unitarity cuts associated with all the energy and subenergy channels of a production process. It is ordinarily considered that the discontinuity equation follows from unitarity and Hermitian analyticity. Recently, Stapp has shown that the discontinuity equation can be derived as a direct consequence of the superposition principle and the in-out boundary conditions for the S matrix, quite independent of unitarity and time reversal invariance.[3] In terms of the scattering function M, defined by $S=I+M$, this equation has the form

$$M(\sigma_i+, s+, \sigma_j'+)-M(\sigma_i-, s-, \sigma_j'-)$$
$$=M(\sigma_i-, s-, \sigma_k''-)M(\sigma_k''+, s+, \sigma_j'+), \quad (1.1)$$

where s is the total energy squared and the σ variables represent the squares of the various subchannel energies. The $\pm$ signs designate $\pm i\epsilon$, and the intermediate variables σ_k'' are to be integrated over the ranges allowed by the phase space of the intermediate state. This is the basic, over-all discontinuity equation. It does not, however, give the discontinuity for any one variable alone, except in the simplest case of a two-

[1] G. F. Chew, *S-Matrix Theory of Strong Interactions* (W. A. Benjamin, Inc., New York, 1961).
[2] H. P. Stapp, Phys. Rev. **125**, 2139 (1962); Lawrence Radiation Laboratory Report UCRL-9875 (unpublished).
[3] H. P. Stapp, Midwest Conference on Theoretical Physics, Notre Dame University, June 1963 (to be published).

particle intermediate channel. Our aim is to derive from (1.1) all the single-variable discontinuity equations of a production amplitude. In the course of the derivation we shall encounter and must solve some of the problems mentioned in the preceding paragraph.

Consider the production process as pictured in Fig. 1(a) and let us use the scalar variables as indicated in that figure. One may ask what the discontinuity across the subenergy σ is. If one assumes that the usual two-particle discontinuity equation can be generalized to this case, the result can be shown pictorially as in Fig. 1(b). (An algebraic formulation will be given later.) Since ω_1 is an energy-like variable and must have a value greater than its two-particle threshold if the production process is physical, certain questions immediately arise. Should ω_1 be evaluated above or below the two-particle unitarity cut? How does the answer depend upon the external variables? Note that these questions do not arise in model calculations,[4] where the interaction between only two of the three particles in the final state is assumed to be dominant.

We propose to derive the discontinuity equation for a subenergy variable by an analytic continuation from a region where the same variable is the total energy of the crossed process, for which the two-particle discontinuity equation is known by virtue of (1.1). In other words we start with the process for which line 3 in Fig. 1 (b) is originally on the same side as lines 1 and 2; then keeping σ fixed above its two-particle threshold, we vary the other variables in such a way that in the end line 3 is effectively swung over to the other side. In effecting this continuation, the main problem is to find all the singularities that may obstruct the path and to determine the appropriate locations of the associated branch cuts, so that one can avoid continuing into unphysical sheets. The implication is, therefore, that one must determine the boundaries of the physical sheet, at least to a certain order in the structure of the singularities. Since, by definition, the physical sheet must contain all the physical points, the boundaries will be so chosen that one can always analytically continue from one physical point to another along paths that stay within the sheet, and that this property is preserved when the singularity structure of higher order is considered. In fact, we shall adopt a rule for the placement of the branch cuts of a discontinuity function by requiring that the form of the discontinuity equation is the same at all points of the "principal" sheet bounded by these cuts. The singularity structure of the scattering function itself can then be determined with the help of Cauchy's theorem.

In Sec. II we present the considerations needed for the determination of the singularities of a scattering function and the boundaries of the principal sheet of the associated discontinuity functions. The considera-
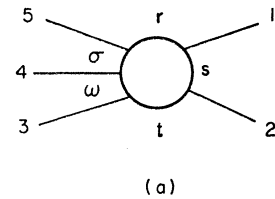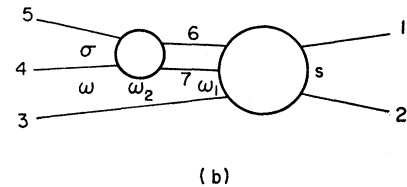
[4] L. F. Cook, Jr., and B. W. Lee, Phys. Rev. **127**, 283, 297 (1962); J. S. Ball, W. R. Frazer, and M. Nauenberg, *ibid.* **128**, 478 (1962); R. C. Hwa, *ibid.* **130**, 2580 (1963).
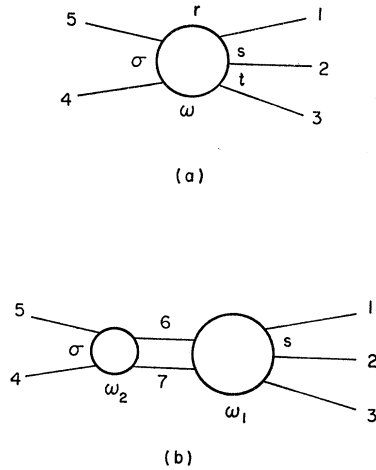

FIG. 1. Production process, with s being the total energy variable.

tions are illustrated by the study of some of the first-order singularities of a production amplitude. Continuation of a two-particle discontinuity function is studied in Sec. III; the discontinuity equation in a subchannel energy variable is then obtained. The problem is later extended in Sec. IV to include singularities of higher order. After the discontinuity equations in subenergy variables are obtained, we then derive (in Sec. IV) the discontinuity across the three-particle cut in the total energy variable with the other variables kept fixed. This is quite simple once we understand the structure of the physical sheet and some properties of the two-particle subenergy discontinuity equations.

II. THE PHYSICAL SHEET

In this section we consider, by means of a simple example, a procedure for determining the boundaries of the physical sheet in accordance with the principle of maximal analyticity. It will be well to state at the outset our interpretation of this principle. We first assume that it is possible to derive from (1.1) single-variable discontinuity equations. Equation (1.1) itself is such an equation in the case of two-particle discontinuity in the s variable. Results of this work (and generalization to more complicated processes to be discussed in a later paper) justify the assumption that single-variable discontinuity equations can be derived in any variable. In conjunction with Cauchy's theorem, such a discontinuity equation allows one to express a certain contribution to the scattering function M in terms of other M functions. We interpret maximal analyticity to mean that M can be built up as a sum of such contributions, plus, perhaps, contributions from contours at infinity. The general procedure for obtaining the analytic structure is to start with contributions coming from the Cauchy contours near the physical region, first without regard to singularities of the M functions on the right of the discontinuity equations,

(a)

FIG. 2. Production process, with σ being the total energy variable.

(b)

and then to introduce the structure of these functions by means of an iteration procedure.[2] The singularities are thereby classified as to order. In this section we examine in detail the singularities obtained by iterating once the discontinuity equation in σ with a pole in ω_1 [see Fig. 1(b)]. There are many other possible singularities of the same order obtainable by iterations with poles (or normal thresholds) in other channels; their properties can be studied in a similar manner.

A. The Starting Point

Let the process shown in Fig. 2(a) be represented by the function[5] $M(s,\sigma,\omega)$. The invariant variables are defined in terms of the momentum four-vectors as follows:

$$s = (k_1 + k_2)^2, \quad \sigma = (k_4 + k_5)^2, \quad \omega = (k_4 - k_3)^2.$$

The two-particle discontinuity equation in the total energy variable σ has a form as given by (1.1). On the right-hand side there is implied an integration over the intermediate phase-space factor, which, for a two-particle intermediate channel of masses m_6 and m_7, is

$$\int \prod_{i=6,7} \left[\frac{d^4 k_i}{(2\pi)^4} 2\pi \delta(k_i{}^2 - m_i{}^2)\theta(k_i{}^0) \right]$$

$$\times (2\pi)^4 \delta^4(k_4 + k_5 - k_6 - k_7). \quad (2.1)$$

The diagram associated with this discontinuity is shown in Fig. 2(b). The normal threshold singularity in the σ variable is located at the point where the above phase-space factor vanishes, i.e., at $\sigma = \sigma_t \equiv (m_6 + m_7)^2$. The discontinuity is nonvanishing only along the real axis for $\sigma > \sigma_t$, provided the external momenta are real[2]; it is only in this case that the energy-momentum conservation laws can be satisfied

---

[5] We shall not exhibit explicitly the dependence of M on the other two variables r and t.

with real internal momenta, and that (2.1) is consequently well defined. The external momenta are guaranteed to be real if the thresholds of the external channels are lower than the internal threshold. Thus, if the masses of the external particles are sufficiently small the Cauchy contour will give a contribution that reduces to a line integral over the discontinuity function extending from σ_t to infinity along the real axis. The position of this contour, which defines a boundary of the physical sheet, will, for large mass values, be determined by continuation in the external masses. The justification of this procedure will be discussed later. Thus, neglecting contributions associated with other possible singularities in the σ plane, we have as our starting point the formula

$$M(s,\sigma,\omega) = \frac{1}{2\pi i} \int_{\sigma_t}^{\infty} \frac{d\sigma'}{\sigma' - \sigma} M_\sigma(s,\sigma',\omega), \quad (2.2)$$

which is valid if the (effective) external masses[6] are small enough. This is the normal or first-order contribution to M associated with this two-particle intermediate state. This contribution will always remain for M, but it may, for larger values of the external masses, be augmented by higher order contributions, which come from possible added segments of the path of integration that detour around cuts of M_σ. Although the normal contributions are called the first-order contributions they are much more comprehensive than the first-order perturbation contributions, as they in fact constitute the entire function for small values of external effective masses.

The discontinuity function M_σ appearing in (2.2) is

$$M_\sigma(s, \sigma'+, \omega) \equiv M(s, \sigma'+, \omega) - M(s, \sigma'-, \omega)$$

$$= \int d\Omega_{\sigma'}\rho(\sigma'+)A(\sigma'-, \omega_2)M(s, \sigma'+, \omega_1), \quad (2.3)$$

where

$$\rho(\sigma') = p_7(\sigma')/32\pi^2(\sigma')^{1/2}. \quad (2.4)$$

Here p_7 is the magnitude of the three-momentum of particle 7 in the rest frame of the σ' channel, and the integration is to be taken over all possible directions of this momentum. $A(\sigma',\omega_2)$ represents the left-hand bubble in Fig. 2(b); $M(s,\sigma',\omega_1)$ represents the right.

The first problem is to determine the locations of the singularities of M_σ in the σ' plane. These are obtained by substituting into the right-hand side of (2.3) various contributions to A and M. One proceeds by iteration, starting with contributions to A and M coming from poles and normal contributions. Contributions with singularities only at very large σ' have no

---

[6] Taking the singularity structure shown in Fig. 3 as example, the variable s is the effective mass of the channel consisting of particles 1 and 2. To ensure real and undistorted Cauchy contour, it is s, $m_3{}^2$, $m_4{}^2$, and $m_5{}^2$ that must be small; the values of $m_1{}^2$ and $m_2{}^2$ individually are unimportant.

singularity structure in the region of small σ' and therefore act in this region effectively as constants with respect to the singularity structure. We shall consider first the singularities of M_σ that are associated with the constant part of A and the pole term

$$M(\omega_1) = \Gamma/(\omega_1 - m_8^2) \qquad (2.5)$$

in M. The corresponding diagram is shown in Fig. 3. We shall insert these contributions into (2.2) for small external masses, then continue the masses to their actual values, and finally study the function M as an analytic function of s and σ. Before so doing, however, we discuss briefly the procedure of continuation in external mass.

B. Continuation in External Mass

The problem of justifying continuation in the masses of external particles within the framework of analytic S-matrix theory has been considered by Stapp.[7] We describe here the main idea.

Suppose we want to continue in m_3 the M function corresponding to the diagram given in Fig. 2(a). Then first consider the M function of a larger process, involving six external particles instead of five; let us call it $M'(s,\sigma,\tau)$ where τ is the effective mass squared of the two particles as indicated in Fig. 4. The analytic structure of M' can be determined in the same way as that of M, and for every contribution to M there will be an analogous contribution to M'. Now, general properties of the analytic S-matrix theory require that M' have a pole at $\tau = m_3^2$. Moreover, the residue at any such pole must be factorizable.[8] In particular,

$$\lim_{\tau \to m_3^2} (\tau - m_3^2) M'(s,\sigma,\tau) = GM(s,\sigma),$$

where G is a constant. It follows that $M(s,\sigma)$ defined in this way can have cuts and singularities only at the limit points of the cuts and singularities of $M'(s,\sigma,\tau)$ as $\tau \to m_3^2$. If $M'(s,\sigma,\tau)$ is analytic in τ as $\tau \to m_3^2$, its singularities in s and σ must move continuously. Thus one can determine the locations of singularities of M by tracing the corresponding singularities of M' as $\tau \to m_3^2$. It is in this sense that we shall discuss continuation in the external masses. Note that we have in no way implied that the actual scattering functions are defined for unphysical values of the masses.
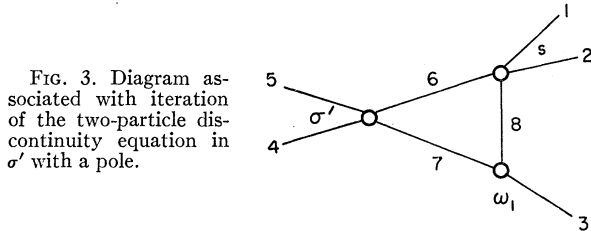

FIG. 3. Diagram associated with iteration of the two-particle discontinuity equation in σ' with a pole.

[7] H. P. Stapp (unpublished).
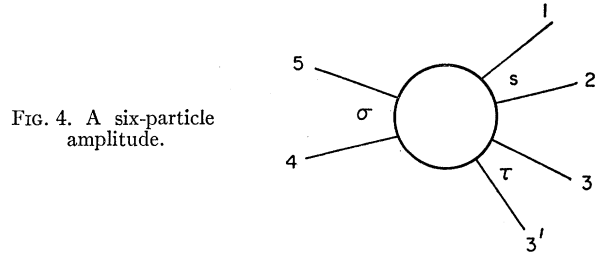[8] D. I. Olive (to be published).

FIG. 4. A six-particle amplitude.

C. Locations of Singularities

We now proceed with the problem of determining the locations of the singularities of $M(s,\sigma)$ corresponding to the diagram in Fig. 3. Define θ as the angle between $\mathbf{k}_3$ and $\mathbf{k}_7$ in the rest frame of the σ' channel. Thus, we have

$$\omega_1 = m_3^2 + m_7^2 - 2E_3 E_7 + 2p_3 p_7 \cos\theta, \qquad (2.6)$$

where

$$E_3 = (\sigma' - s + m_3^2)/2\sigma'^{1/2},$$
$$E_7 = (\sigma' - m_6^2 + m_7^2)/2\sigma'^{1/2}, \qquad (2.7)$$
$$p_3 \equiv |\mathbf{k}_3| = (E_3^2 - m_3^2)^{1/2},$$
$$p_7 \equiv |\mathbf{k}_7| = (E_7^2 - m_7^2)^{1/2}.$$

Equation (2.3) may now be written in the form

$$M_\sigma(s,\sigma') = g(s,\sigma') \int_{-1}^{1} \frac{dz}{z - \beta(s,\sigma')}, \qquad (2.8)$$

where

$$z \equiv \cos\theta, \quad g(s,\sigma) = \pi A \Gamma \rho(\sigma)/p_3(s,\sigma) p_7(\sigma), \qquad (2.9)$$

$$\beta(s,\sigma) = [m_8^2 - m_3^2 - m_7^2 + 2E_3(s,\sigma) E_7(\sigma)]/2p_3(s,\sigma) p_7(\sigma), \qquad (2.10)$$

or

$$\beta(s,\sigma)$$
$$= [\sigma^2 - \sigma(s + m_3^2 + m_6^2 + m_7^2 - 2m_8^2) + (s - m_3^2)(m_6^2 - m_7^2)]$$
$$\times \{[\sigma - (s^{1/2} + m_3)^2][\sigma - (s^{1/2} - m_3)^2]$$
$$\times [\sigma - (m_6 + m_7)^2][\sigma - (m_6 - m_7)^2]\}^{-1/2}. \qquad (2.11)$$

Since $A(\sigma',\omega_2)$ is a constant here, (2.8) has no dependence on ω. A discussion of the relaxation of this restriction is given in Sec. IV.

The singularities of $g(s,\sigma')$ are located at $(\sigma'^{1/2} \pm m_3)^2$ in the s plane and at $(s^{1/2} \pm m_3)^2$ in the σ' plane. The integral in (2.8) also has square-root branch points at these positions, which cancel the singular behavior of $g(s,\sigma')$, resulting in the fact that $M_\sigma(s,\sigma')$ is regular there. This is, of course, true only in the principal branch of the logarithm coming from the integration. In addition, the integral has square-root branch points $\sigma' = (m_6 \pm m_7)^2$, which are in $M_\sigma(s,\sigma')$ also.

$M_\sigma(s,\sigma')$ has, furthermore, the end-point singularities, which occur when

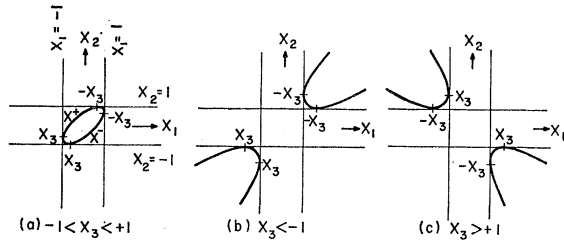$$\beta(s,\sigma') = \pm 1. \qquad (2.12)$$

FIG. 5. Real sections of the singularity surface for
three different ranges of values of x_3.

Using (2.11), it can be shown that (2.12) can be
satisfied only by $\sigma'=0$, ∞ and by the roots of

$$f(s,\sigma')=0, \qquad (2.13)$$

where

$$
\begin{aligned}
f(s,\sigma) &= s\sigma m_3{}^2 + s^2 m_7{}^2 + \sigma^2 m_8{}^2 + m_3{}^2 m_6{}^2 \\
&\quad - s\sigma(m_7{}^2+m_8{}^2) - sm_3{}^2(m_6{}^2+m_7{}^2) - \sigma m_3{}^2(m_6{}^2+m_8{}^2) \\
&\quad + s(m_7{}^2-m_8{}^2)(m_7{}^2-m_6{}^2) + \sigma(m_8{}^2-m_6{}^2)(m_8{}^2-m_7{}^2) \\
&\quad + m_3{}^2(m_6{}^2-m_7{}^2)(m_6{}^2-m_8{}^2).
\end{aligned}
$$

It is straightforward to establish the equivalence of
(2.13) to the following equation,

$$x_1{}^2+x_2{}^2+x_3{}^2+2x_1x_2x_3-1=0, \qquad (2.14)$$

where

$$x_1 = (\sigma'-m_6{}^2-m_7{}^2)/2m_6m_7,$$

$$x_2 = (s-m_6{}^2-m_8{}^2)/2m_6m_8,$$

$$x_3 = (m_3{}^2-m_7{}^2-m_8{}^2)/2m_7m_8.$$

This equation has been derived previously[9] by examin-
ing the analytic property of the Feynman amplitude
for a triangle diagram in the perturbation theory. The
derivation here is based on the consideration of the
pole contribution to the discontinuity equation accord-
ing to the iteration procedure in the analytic S-matrix
theory.

From (2.13) we see that there are two singularities
in the σ' plane whose positions depend on s and m_3;
let us denote them by $\sigma_\pm(s,m_3)$. They are given by

$$x_1{}^\pm = -x_2x_3 \pm (x_2{}^2-1)^{1/2}(x_3{}^2-1)^{1/2}. \qquad (2.15)$$

If the value of x_3 is in the interval $(-1, +1)$, the real
solutions of x_1 as a function of real x_2 form an ellipse
inside the square whose sides are $x_1=\pm 1$ and $x_2=\pm 1$;
this is shown in Fig. 5(a). If $|x_3|>1$, then the inter-
section of the solution surface with the real x_1-x_2
plane is a hyperbola, as indicated in Figs. 5(b) and
(c). In all cases, the points of tangency with the lines
$x_1=\pm 1$ and $x_2=\pm 1$ are $+x_3$ or $-x_3$.

The starting point of the study is at small values of
s and $m_3{}^2$; thus, x_2 and x_3 may be taken to be less than
-1 initially. We increase $m_3{}^2$ to its physical value

[9] R. J. Eden, Lectures in Theoretical Physics, Brandeis Summer
Institute, 1961 (W. A. Benjamin, Inc., New York, 1962), Vol. 1.

first, and then study the analytic structure of $M_\sigma(s,\sigma')$
in the two variables s and σ'. We assume that the
physical value of $m_3{}^2$ satisfies the stability constraints
$|m_7-m_8|<m_3<m_7+m_8$. The corresponding value of
x_3 is therefore restricted to the interval $(-1, +1)$. In
the continuation of x_3 from a value less than -1 to a
value in the interval $(-1, +1)$, the solution curve for
$x_1{}^\pm(x_2,x_3)$ changes gradually from a hyperbola [Fig.
5(b)] to a straight line (when $x_3=-1$) and then to an
ellipse [Fig. 5(a)]. The branch points $x_1{}^\pm(x_2,x_3)$ in the
x_1 plane for $x_2<-1$ are initially real and not greater
than -1; this means that in the σ' plane the singulari-
ties are below the normal threshold σ_t while the σ'
integration contour lies undistorted along the real axis
from σ_t to $+\infty$. As the hyperbola becomes a straight
line $x_1{}^\pm=x_2$, the branch points $\sigma_\pm(s,m_3)$ coincide at a
real point below σ_t, still leaving the contour undistorted.
As the straight line develops into an ellipse, these
singularities go into the complex σ' plane taking con-
jugate positions.

This is the situation from which we start investi-
gating the analyticity of $M(s,\sigma)$ with all the external
masses having physical values. The value of s at this
point is small. Let us now increase s along a path just
above the real axis, as shown in Fig. 6(a). The tra-
jectories of the singularities $\sigma_\pm(s)$ of $M_\sigma(s,\sigma')$ in the
σ' plane are as indicated in Fig. 6(b). Corresponding to
$x_2=-x_3$ is the point

$$
\begin{aligned}
s=s_1 &= m_6{}^2+m_8{}^2+m_6m_7+m_6(m_8{}^2-m_3{}^2)/m_7 \\
&< (m_6+m_8)^2;
\end{aligned}
$$

at this point $\sigma_-(s)$ reaches the threshold σ_t which is the
lower limit of the integration in the dispersion formula
(2.2). However, $M(s,\sigma)$ has no end-point singularity at
s_1, as can be verified by taking the two possible ways
of continuing s around s_1 and showing that the differ-
ence is zero. Continuation past s_1 with a small positive
imaginary part has the result that $\sigma_-(s+)$ goes around
σ_t in the clockwise direction, dragging the dispersion
contour with it as it retreats. Corresponding to $x_2=+1$
is $s=s_t=(m_6+m_8)^2$, where $\sigma_\pm(s)$ meet and pinch the
contour; indeed, s_t is a branch point of $M(s,\sigma)$. Clock-
wise continuation in s around s_t leads $\sigma_-(s+)$ to the
lower half σ' plane, so the σ' contour is distorted
downward. The trajectories of $\sigma_\pm(s-)$ are complex
conjugate to those of $\sigma_\pm(s+)$. For $s>s_t$, the deforma-
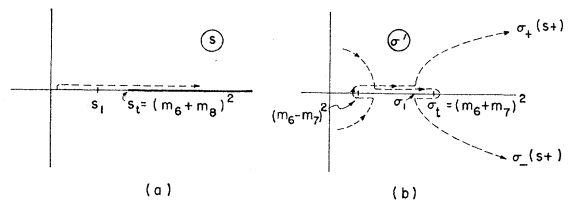tions of the dispersion contour are shown in Figs.

FIG. 6. (a) Path of continuation in s; (b) the corresponding trajec-
tories of the singularities in the σ' plane.

7(a) and (b) for the two cases of $s+i\epsilon$ and $s-i\epsilon$. We remark that the distortion is forced by the movement of the singularity $\sigma_-(s)$; the particular way in which the contour in Fig. 7 is drawn is not meant to imply an appropriate position of the branch cut ending at $\sigma_-(s)$, which is as yet undetermined.

When s is sufficiently small, the dispersion contour in the σ' plane is along the real axis undistorted. This contour in σ' corresponds to a branch cut in $M(s,\sigma)$ along the real axis of σ plane for $\sigma>\sigma_t$, across which the discontinuity M_σ is nonvanishing. Physical region is just above this cut. For the process indicated in Fig. 2(b), this region is at values of σ greater than $\max\{(m_4+m_5)^2, (s^{1/2}+m_3)^2, \sigma_t\}$. When s is sufficiently large, there is also another region above the cut on the real axis, which is also physical, corresponding to the process shown in Fig. 1(b). The bounds of this region are $\max\{(m_4+m_5)^2, \sigma_t\}$ on the lower end and $(s^{1/2}-m_3)^2$ on the upper end. For the convenience of discussion, we define two sheets, I and II, of $M(s,\sigma)$, connected by the branch cut on the real σ axis. Since σ_t is a two-particle threshold, this cut connects only two sheets and no more. Let sheet I contain the physical points above the cut; hence, it must contain also the physical sheet. Conversely, the unphysical sheets must contain sheet II.

We can now give the locations of the moving singularities of $M(s,\sigma)$ in sheets I and II of the σ plane for fixed s. They are at those points where the pole in the integrand of (2.2) pinches the contour of integration with the singularities $\sigma_\pm(s)$ of $M_\sigma(s,\sigma')$. Since the pole $(\sigma'-\sigma)^{-1}$ appears as a multiplicative factor in the integrand, it is on all sheets of σ' defined by branch cuts of $M_\sigma(s,\sigma')$. We find therefore with the help of Fig. 7 that, for $s+i\epsilon$, $\sigma_-(s+)$ is in the lower half of the σ plane in sheet I, while $\sigma_+(s+)$ is in the upper half of sheet II. For $s-i\epsilon$, $\sigma_-(s-)$ [$\sigma_+(s-)$] is in the upper (lower) half of sheet I (II).

Singularities of $M(s,\sigma)$ in the s plane for fixed σ can be found in a similar way. Let the solutions of (2.13) for fixed σ' be denoted by $s_\pm(\sigma')$. Then, because of the symmetry of Fig. 5 under interchange of x_1 and x_2, the trajectories of $s_\pm(\sigma')$ are analogous to those shown in Fig. 6 except that the roles of s and σ' are interchanged. Let us use the notation in which $s_+(\sigma')$ is associated with the solution of $\sigma'=\sigma_+(s)$, and $s_-(\sigma')$
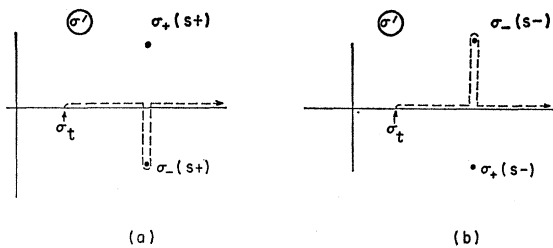

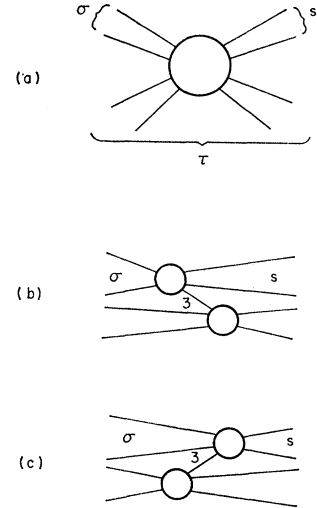FIG. 7. Distortions of the contour of integration of the dispersion formula.

FIG. 8. (a) An eight-particle amplitude; (b) and (c) a pole in τ in two different physical regions.

with $\sigma'=\sigma_-(s)$. Sheets I and II can be defined in a similar way as before. They are connected by the branch cut on the real axis of the s plane starting from $s_t=(m_6+m_8)^2$ to $+\infty$. The singularities of $M(s,\sigma)$ are then located as follows: for $\sigma+i\epsilon$ where $\sigma>\sigma_t$, $s_-(\sigma+)$ is in the lower half of sheet I, while $s_+(\sigma+)$ is in the upper half of II. For $\sigma-i\epsilon$, $s_-(\sigma-)$ is in the upper half of sheet I and $s_+(\sigma-)$ is in the lower half of sheet II.

D. Placement of Branch Cuts

Having found the locations of the branch points, we now proceed to investigate the appropriate choice of the positions of the branch cuts connected to these singularities. Consider the σ plane for s fixed at a value greater than s_t and just above the real axis. Aside from the normal threshold the only singularity of $M(s,\sigma)$ on sheet I is $\sigma_-(s+)$ in the lower half-plane. Since this singularity enters into sheet I by emerging through the branch cut on the real axis in a downward direction, it is natural to take the branch cut attached to it to connect to the lower side of the cut along the real axis. A necessary condition that the position of any branch cut must satisfy is that the resultant physical sheet contains all the physical points. If the physical regions corresponding to the two physical processes represented by Figs. 1 and 2 are analytically connected by a path that runs on a straight line just above the real axis of the σ plane, then any branch cut connecting to the bottom of the normal cut would be acceptable, at least as far as these two regions are concerned. In order to determine whether a straight path of continuation just above the real axis, in fact, leads from one physical region to another, one must have some criterion for determining in general the analytic connection between various physical regions. We discuss this question now.

Consider the scattering process of four particles into four particles, and denote its function by $M(s,\sigma,\tau)$,
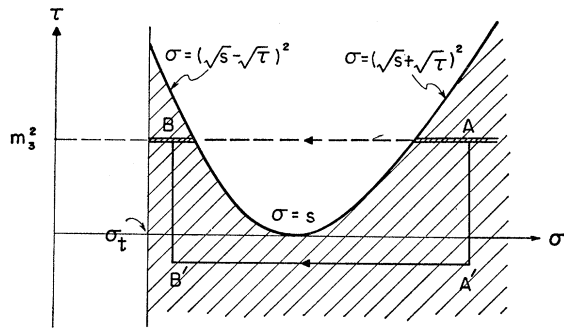
FIG. 9. A section of the physical region
of the eight-particle amplitude.

where τ is as indicated in Fig. 8(a). For s large enough and τ positive, there are two physical regions in the σ plane above the real axis. Let us call the lower region B, which ranges from $\max\{(m_4+m_5)^2, \sigma_t\}$ to $(s^{1/2}-\tau^{1/2})^2$, and call the upper region A, which extends from $(s^{1/2}+\tau^{1/2})^2$ to $+\infty$. When τ is reduced, the gap separating the two regions narrows, and when τ becomes negative, A and B become connected. For fixed $s+i\epsilon$, the physical region of $M(s,\sigma,\tau)$ as a function of σ and τ is shown in Fig. 9. Now, it can be shown[7,8] that the presence of a pole at $\tau=m_3^2$ of $M(s,\sigma,\tau)$ in the physical region is the necessary and sufficient condition for the existence of a physical particle of mass m_3^2. Moreover, the residue of such a pole must factorize into two factors, which are scattering amplitudes. Poles in regions A and B correspond to processes represented in Figs. 8(b) and (c), respectively.

In Fig. 9 a path of continuation staying in or very near the physical region defines the connection between the physical regions A and B. Such a path is shown by the solid line. A continuation of the eight-particle amplitude from A to B with τ staying at the pole position at all times is indicated by the dashed line in Fig. 9; it must necessarily pass through an unphysical region. By virtue of the factorizability of the residue, the analytic structure of the eight-particle amplitude at the pole is composed of the analytic structures of the two-component five-particle amplitudes. The continuation along the dashed line in Fig. 9 is achieved by continuing the component amplitudes in their own variables, along paths not yet determined. The question is whether such a path exists. If it does, then the existence of a pole at $\tau=m_3^2$ in one of the two regions, A or B, must imply the existence of the pole in the other region as well. This then implies the existence of a second particle of mass m_3^2, which may be identified as the antiparticle. It is in this way that the existence of the antiparticle follows from S-matrix principles. Moreover, the path of continuation from A to B that stays at $\tau=m_3^2$ defines the continuation from the original region to the cross-process region for the five-particle scattering amplitudes appearing in Figs. 8(b) and (c).

The above conclusions follow if one can find a path from A to B that stays at $\tau=m_3^2$. The problem, then, is to construct such a path. The way to do this is to take the path from A' to B' in Fig. 9, which is at a negative value of τ and which lies in or very near the physical region, and to gradually increase τ. For the singularities that will be present in the five-particle amplitudes this continuation is just the continuation in τ that was already considered. Thus the connection between the two physical regions of the five-particle amplitude is defined by a path of continuation obtained by distorting the straight line above the real σ axis at $\tau<0$ in such a way as to avoid singularities that emerge when τ is increased to m_3^2. The path defined in this way will give a path in the eight-particle amplitude that is (homotopically) equivalent to the original path from A to B via A' and B', as is required.

Consider the present specific example. When τ is negative, there is no unphysical gap separating physical regions in the σ plane, as we have already noted. Thus, the path of continuation may be placed just above the real axis, imbedded in the physical region. By considerations similar to those given in the preceding subsection, the singularities $\sigma_\pm(s+)$ can be found to be located in sheet II just above the real axis. As τ is increased to a positive value, the physical region breaks up into two disjointed sections A and B. The singularities $\sigma_\pm(s+)$ become complex for $\tau>(m_7-m_8)^2$; $\sigma_+(s+)$ goes to the upper half-plane of sheet II, while $\sigma_-(s+)$ goes through the real axis and enters into the lower half-plane of sheet I. Neither of these singularities disturbs the path of continuation between A and B just above the real σ axis in sheet I. There is no need to consider the singularities associated with $s-i\epsilon$, since the physical regions are for $s+i\epsilon$. Hence, to the extent of first-order iteration of the discontinuity equation in σ, no singularity of $M(s,\sigma)$ deforms the straight path of continuation between A and B. These regions will both be on the physical sheet if the branch cut attached to $\sigma_-(s+)$ is taken connected to any point on the lower side of the normal cuts along the real axis.

The above arguments do not specify the exact point of the real axis at which the exit point should lie. In Fig. 10(a) we show two possible positions of the complex branch cut in the σ plane. Clearly, the discontinuity across the real axis is the same in the two cases except along the segment bounded by the two alternative exit points. Neither choice is incorrect, but one particular location is more convenient than the other. We establish the following rule: The branch cuts of the discontinuity function associated with singularities arising from iteration of the discontinuity equation are to be placed along the images of the real interval $[-1, +1]$ of $\cos\theta$ under the appropriate mapping, which in the present example is the inverse of $\cos\theta$ $=\beta(s,\sigma')$, as defined by (2.11). Let us refer to these images as the "natural" positions of the branch cuts, and the sheet of the discontinuity function defined by

these natural branch cuts as the "principal" sheet. The generalization to more complicated problems is rather clear: the natural positions of the boundaries of the principal sheet are such that on this sheet the phase-space integrations of a discontinuity equation are never distorted by the singularities of the M functions in the integrand, which of course move as one changes the external parameters. Any distortions of the contour of integration in (2.2) will be taken to run along these cuts. The physical sheet defined by this representation will therefore have, in addition to the normal cut, possible added cuts that will run along positions of these (natural) cuts that bound the principal sheet.

For our example the physical sheet defined in this way certainly satisfies the homotopy condition. The natural position of the complex branch cut of $M_\sigma(s+,\sigma')$ in the σ' plane connects $\sigma_-(s+)$ with $\sigma_+(s+)$, as shown approximately in Fig. 10(b). Since the dispersion contour is distorted downward for $s+i\epsilon$ [cf. Fig. 7(a)], the resultant branch cut of $M(s+,\sigma)$ in the σ plane is in the lower half of sheet I, as indicated by the solid curve in Fig. 10(a). That the homotopy requirement will always be satisfied by this rule for placing cuts remains to be established.

The rule has many advantages. Firstly, the second-type singularities,[10] corresponding to internal momenta being distorted to infinity, must be on an unphysical sheet. This is because integrations over undistorted, real internal momenta correspond to phase-space integration taken over physical angles, and a second-type singularity occurs when some contour of this integration is distorted to infinity, as we shall see in the next section. Secondly, the natural position of the complex cut of $M_\sigma(s,\sigma')$ in our example intersects with the real axis at a point between $(s^{1/2}-m_3)^2$ and $(s^{1/2}+m_3)^2$ [see Fig. 10(b)]; consequently, at least in the order considered, the discontinuity functions in the physical regions A and B never have discontinuities themselves in the same variable σ'. The position of this exit point can be found by recognizing that the point of intersection corresponds to $\beta(s,\sigma')=0$, whose solution, according to (2.10), is

$$E_3(\sigma') = (m_3^2 + m_7^2 - m_8^2)/2E_7(\sigma').$$

Since E_7 is greater than m_7 if $\sigma' > \sigma_t$, and m_3^2 is restricted by stability constraints, E_3 must be less than m_3, thus limiting the intersection point to be within the unphysical gap between A and B. Thirdly, the boundaries of the physical sheet determined by this rule make possible an integral representation[11] of the production amplitude involving real contours only. To achieve this, conformal transformations on some of the variables are clearly needed. Lastly, the discontinuity equations in the physical regions are simple, as we shall see in the following sections.

[10] D. B. Fairlie, P. V. Landshoff, J. Nuttall, and J. C. Polkinghorne, J. Math. Phys. 3, 594 (1962).
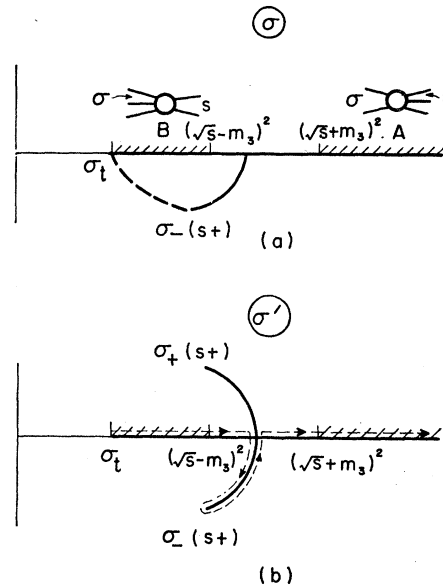[11] R. C. Hwa (unpublished).

Fig. 10. (a) Two alternative positions of the complex branch cut of M function in the σ plane. (b) Distortion of the σ' contour of integration by the natural position of the complex branch cut of M_σ in the σ' plane.

Adopting this rule, we make several comments concerning the natural positions of the branch cuts of $M(s,\sigma)$. Because (2.11) can be put in the form of a fourth-order algebraic equation in σ' with real coefficients if s is real, the natural cuts of $M_\sigma(s,\sigma')$ in the σ' plane must have mirror symmetry about the real axis, as we have indicated in Fig. 10(b). For $M(s+,\sigma)$, the lower half of the cut joining $\sigma_-(s+)$ with $\sigma_+(s+)$ is in sheet I, the upper half being in sheet II, and vice versa for $M(s-,\sigma)$. In both cases there is another cut in the unphysical sheet connecting $\sigma=0$ with $-\infty$ along some path which may have complex parts. The situation in the s plane is similar and will not be described in detail here. We mention only that if σ is large enough, there are also two physical regions in the s plane just above the real axis. The lower region is bounded by $\max\{s_t, (m_1+m_2)^2\}$ on the lower end and by $(\sigma^{1/2}-m_3)^2$ on the upper end. It is physical for the process of Fig. 2(b), and should therefore be labeled A. The higher region is for $s > (\sigma^{1/2}+m_3)^2$; it is labeled B, since it is the physical region of the process indicated in Fig. 1(b). The normal position of the branch cut of $M_\sigma(s,\sigma')$ for $\sigma' > \sigma_t$ is also arched; it intersects the real s axis in the gap between A and B.

III. THE DISCONTINUITY EQUATIONS

In the immediately preceding section we have given a rule for the placement of branch cuts of discontinuity functions, compatible with the homotopy condition on paths of continuation between physical points. These natural positions of the branch cuts define the principal sheet, which has the property that at any point
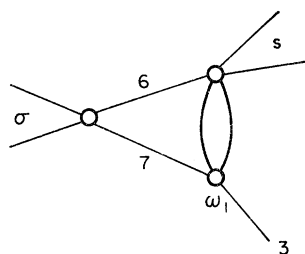
FIG. 11. Diagram associated with iteration of M_σ with a two-particle normal cut in ω_1.

on this sheet the normal, real integrations over phase space in the discontinuity formulas are not distorted. In this section we derive the discontinuity equation for the production amplitude $M(s,\sigma,\omega)$ in the subchannel energy σ by an analytic continuation in s, for fixed σ, from the region (A) where the crossed process (σ being the total energy) is physical, and where we know what the discontinuity in σ is. In particular, we want to answer the questions raised in Sec. I, regarding the sign of the small imaginary part of ω_1 in $M(s,\sigma',\omega_1)$ in (2.3).

In the specific example considered in the preceding section, where the discontinuity equation in σ' is iterated with a pole in the ω_1 channel, we find that the complex branch cut has its natural position in between the two physical regions A and B in the s plane. The discontinuity equation in σ' in region A where $\sigma' > \max\{(s^{1/2}+m_3)^2, (m_4+m_5)^2, \sigma_t\}$ is given by (2.3); in this region the contribution to the dispersion formula for $M(s,\sigma)$ is on the real σ' axis and is undistorted because the external momenta are real. Since, by definition, the discontinuity function on the principal sheet is given by the normal form of the discontinuity equation, we can continue $M_\sigma(s,\sigma')$ in s to region B where $s > (\sigma'^{1/2}+m_3)^2$ along any path in the principal sheet and obtain the result that (2.3) is also valid there. The sign of $\pm i\epsilon$ for ω_1 in the integrand of (2.3) is immaterial even for s in B, since the pole in ω_1 that is considered is not near the (physical) region of integration. This will become evident later, as we consider other singularities in the ω_1 variable.

We now consider the singularities that are associated with the normal two-particle contribution to the function M appearing on the right-hand side of (2.3). That is, instead of a pole, we take $M(s,\sigma',\omega_1)$ in (2.3) to have the form

$$M(s,\sigma',\omega_1)=\frac{1}{\pi}\int_{\omega_t}^{\infty}\frac{d\omega_1'}{\omega_1'-\omega_1}M_{\omega_1}(s,\sigma',\omega_1'),\quad (3.1)$$

where ω_t is the lowest two-particle threshold and M_{ω_1} is the discontinuity across the associated two-particle branch cut on the real axis of the ω_1 plane. The diagram for this case is shown in Fig. 11. Putting (3.1) in (2.3), and ignoring the singularity structure of $A(\sigma',\omega_2)$, as before, we have

$$M(s,\sigma')=g(s,\sigma')\int_{-1}^{1}dzF(s,\sigma',z).\quad (3.2)$$

Here $F(s,\sigma',z)$ has a square-root branch point at $z=\beta'(s,\sigma')$, where $\beta'(s,\sigma')$ is given by (2.11) with $m_8{}^2$ replaced by ω_t. The integral is therefore singular when $\beta'(s,\sigma')=\pm1$. Let the moving singularities in the σ' plane be called $\sigma_\pm'(s)$; their positions may be found by solving (2.14) where, again, $m_8{}^2$ is to be replaced by ω_t.

If ω_t is less than $(m_3+m_7)^2$, which is the ω_1 threshold of the external lines of $M(s,\sigma',\omega_1)$, and if s is greater than s_t, then as before we have $x_2 > +1$, and $-1 < x_3 < 1$, so the singularities $\sigma_\pm'(s)$ are at conjugate points in the complex σ' plane. The natural position of the cut joining them intersects the real axis in the unphysical gap between A and B.

When ω_t becomes equal to $(m_3+m_7)^2$, x_3 becomes -1, and (2.15) becomes simply $x_1{}^\pm=x_2$. Thus, $\sigma_\pm'(s)$ coincidence for all values of s. For s greater than the three-particle threshold $s_t'=(m_3+m_6+m_7)^2$, $\sigma_\pm'(s)$ are greater than σ_t. The image of the point $\beta'(s,\sigma')=0$ in the σ' plane is on the real axis between $(s^{1/2}-m_3)^2$ and $(s^{1/2}+m_3)^2$, as before. It can be verified that the natural position of the branch cut connecting $\sigma_\pm'(s)$ is a closed loop, as shown approximately in Fig. 12. If s is above the cut on the real axis, then the contour of integration in the dispersion representation (2.2) is distorted downward, also shown in the figure. Otherwise, for $s-i\epsilon$, the contour is distorted upward. It is easy to see that no singularity of $M(s,\sigma)$ can be in the physical region, since the contour cannot be pinched there.

Let us now fix σ' at a point σ_0' in region A and determine the natural branch cuts of $M_\sigma(s,\sigma')$ in the s plane. It is not difficult to obtain the result; we sketch it in Fig. 13. The natural complex cut in the s plane also forms a closed loop, enclosing the threshold $(\sigma'^{1/2}+m_3)^2$ of the physical region B. The singularity $s_-'(\sigma')$, given by

$$s_-'(\sigma')=\sigma'(1+m_3/m_7)+m_3(m_3+m_7-m_6{}^2/m_7),$$

is located in region B. It divides the physical region into two sections: B_1 where $s > s_-'(\sigma')$, and B_2 where $(\sigma'^{1/2}+m_3)^2 < s < s_-'(\sigma')$. The section B_2 is inside the loop cut.

We are now in a position to examine the continuation of the discontinuity formula from the region A, where it is originally given, to the region B corresponding to the crossed reaction. For the discontinuity
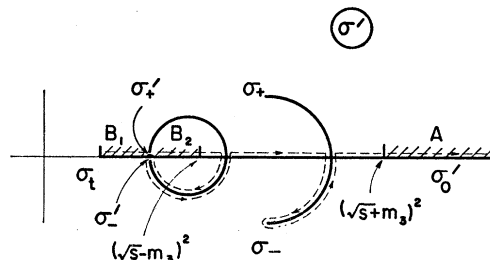

FIG. 12. Principal sheet of $M_\sigma(s,\sigma')$ in the σ' plane for fixed $s+ > (m_3+m_6+m_7)^2$.

function evaluated at σ_0', a continuation in s from A to B that stays on the principal sheet of the discontinuity function, as shown in Fig. 13, will leave the form of the discontinuity at σ_0' unchanged; this is how the principal sheet of $M_\sigma(s,\sigma')$ was defined. One can follow the corresponding motion of the cuts in the σ' plane as they move to the right; these cuts must avoid the fixed point σ_0', since the path of continuation in s detours around the natural branch cuts in the s plane.

Since the contour of integration in the Eq. (3.2) for the discontinuity function is undistorted, it lies along the real interval $[-1, +1]$ in the z plane. In this plane there is a pole and a branch cut belonging to $F(s,\sigma',z)$. The positions of these singularities depend on the values of s and σ' and are guaranteed not to distort the real contour of integration, as long as s and σ' stay on the principal sheet. However, we shall need to know the positions of these singularities and associated cuts relative to the contour of integration, in order to determine the sign of $\pm i\epsilon$ of the argument ω_1 appearing in the discontinuity equation (2.3).

Let us consider the movement of the branch point $\beta'(s,\sigma')$ in the z plane. The value of σ' is fixed at σ_0', so we have $p_7>0$ and $E_7>p_7$. Initially, s is in region A, and so we have $E_3>p_3>0$. Substituting $m_s^2 \to \omega_t \equiv (m_3+m_7)^2$ into (2.10), we find that $\beta'(s,\sigma')$ is real, positive and greater than $+1$, when s is in A. The cut in the ω_1 plane starting at $\omega_1=\omega_t$ maps into a cut in the z plane, running from that value of $\beta'(s,\sigma')$ to $+\infty$, and hence never passes near the interval $[-1, +1]$. Consequently, sign of $\pm i\epsilon$ on ω_1 is immaterial in this region. Now we continue in s to the region B_1, taking a path[12] as shown in Fig. 14(a). With the help of the formula for $\beta'(s,\sigma')$, i.e., (2.11) with $m_8=m_3+m_7$, we find that the image of this path in the z plane is as shown by the dashed line in Fig. 14(b). The segment along the straight line between $[(\sigma_0')^{1/2}-m_3]^2$ and $[(\sigma_0')^{1/2}+m_3]^2$ is mapped onto the negative imaginary z axis. The part just above the loop cut corresponds to the section just below $[-1, 0]$ in the z plane, as it
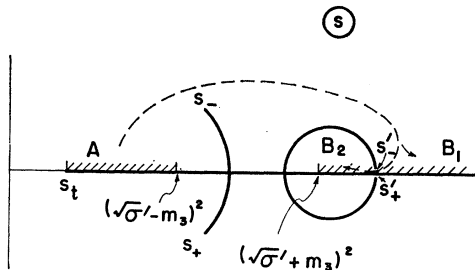

FIG. 13. Principal sheet of $M_\sigma(s,\sigma')$ in the s plane for fixed $\sigma'=\sigma_0'$.

---

[12] Strictly, the proper path in the s plane should avoid the "moon" cut of Fig. 13, which arises on account of the pole iteration; however, so far as the movement of the branch point β' in the z plane is concerned, this is an unnecessary and irrelevant complication and can be ignored.
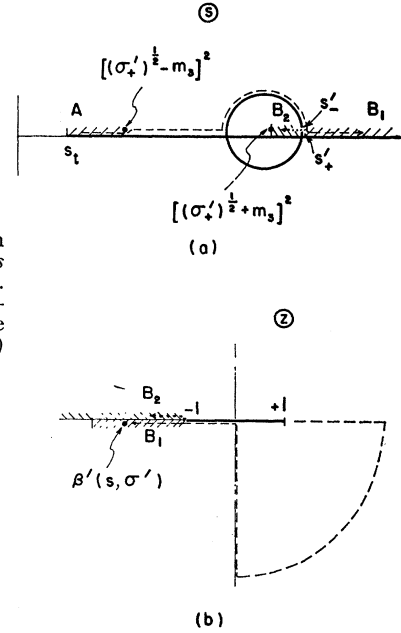

FIG. 14. (a) A path of continuation in s in the principal sheet. (b) The corresponding path of the branch point $\beta'(s,\sigma')$ in the z plane.

is required. The region B_1 is therefore mapped onto the region just below the negative real z axis between $\beta'(\infty, \sigma_0')$ and -1, where

$$\beta'(\infty, \sigma_0') \equiv -(\sigma_0'-m_6^2+m_7^2)$$
$$\times\{[\sigma_0'-(m_6+m_7)^2][\sigma_0'-(m_6-m_7)^2]\}^{-1/2}.$$

On account of (2.6), we see that $\omega_1=+\infty$ goes over to $z=+\infty$ for $p_3>0$, whether s is in region A or B, but it corresponds to $z=-i\infty$ for $[(\sigma_0')^{1/2}-m_3]^2 <s<[(\sigma_0')^{1/2}+m_3]^2$. Hence, when s is continued to region B_1, the branch cut in the z plane runs from $\beta'(s+, \sigma_0')$ to $+\infty$, passing the real interval $[-1, +1]$ on its lower side. The integration of z in (3.2) should, therefore, be above the branch cut of $F(s,\sigma',z)$ in z. See Fig. 15(a). Transformation to the ω_1 variable by (2.6) yields the result that in (2.3) the integration is to be performed over a range of values of ω_1 which should be evaluated above the two-particle branch cut of $M(s+, \sigma'+, \omega_1)$. See Fig. 15(b). That is, ω_1 should be specified by $\omega_1+i\epsilon$. It is to be emphasized that this is true no matter which sign of $\pm i\epsilon$ is associated with ω (the external variable), so long as we have $s+i\epsilon$. Furthermore, it can be shown by the same method that for $s-i\epsilon$ we must use $M(s-, \sigma'+, \omega_1-)$ in (2.3). These properties turn out to be crucial to the derivation of the discontinuity across s, as we shall show in the next section.

Consider now the continuation to region B_2 in the interior of the loop by passing through an infinitesimal gap between $s_\pm'(\sigma')$ made possible by letting ω_t be $(m_3+m_7-\epsilon)^2$. A path leading from B_1 to B_2, as indicated by the dotted line in Fig. 14(a), then maps into a path in the z plane starting from just below the
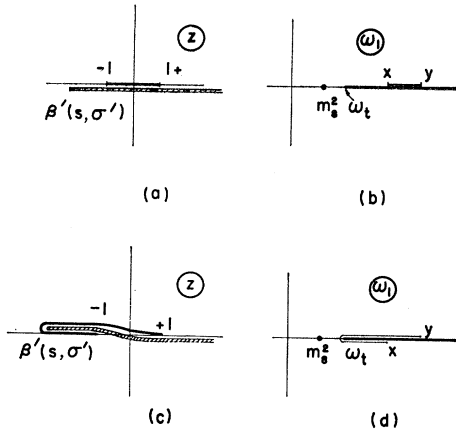
FIG. 15. Ranges of integration of M_σ relative to the branch cut of the integrand for the various cases.

negative real axis; it leads up to $-1-\epsilon$ and then retreats to lower values above the real axis *without* going around $z=-1$ point. Hence, for s in B_2 on the principal sheet, Figs. 15(a) and (b) are still applicable. Throughout the whole region B, therefore, the discontinuity equation in σ' should read

$$M_0(s\pm, \sigma'+, \omega) = h(s\pm, \sigma'+)$$

$$\times \int_x^y d\omega_1 A(\sigma'-, \omega_2) M(s\pm, \sigma'+, \omega_1\pm), \quad (3.3)$$

where $h(s,\sigma') = \pi p(\sigma')/p_3 p_7$, and x and y are physical minimum and maximum values of ω_1 for a fixed total energy $s > (\sigma'^{1/2} + m_3)^2$ and a fixed subenergy $\sigma' > \sigma_t$. The simplicity of the equation is a consequence of the choice of natural position for the branch cut. The price to be paid is that the integral formula for $M(s,\sigma)$ has complex parts.

Suppose we do not take the contour of integration in Fig. 12 to be distorted by the complex natural cut, but collapse the branch cut and take the contour to be straight, lying just above the real axis (ignoring the moon cut due to pole iteration) but below the collapsed cut. This collapsed cut runs from $\sigma_\pm'(s+)$ to $[(s+)^{1/2} - m_3]^2$, which is a singular point as will become clear later. Let the section beneath this cut and above the real axis be denoted by B_2'. The corresponding region in the s plane is reached by approaching the real axis between $[(\sigma'+)^{1/2} + m_3]^2$ and $s_-'(\sigma'+)$ from above by collapsing the loop cut in Fig. 13. Now, it is clear from Figs. 14(a) and (b) that the interior of the loop cut in the s plane maps onto the upper half z plane under the transformation $z = \beta'(s,\sigma')$ for fixed $\sigma' > \sigma_t$. A continuation that distorts the natural cut and thereby leads to the region that is originally on the inside of the cut has the result that β' goes through the interval $[-1, +1]$ on the real axis from below and enters into the upper half-plane. This means that in

the z plane the contour of integration from -1 to $+1$ must be deformed upward. Thus, to reach B_2' in the s plane by collapsing the loop from above, the branch point β' in the z plane must go to the negative real axis $-\infty < z < -1$ by dragging the integration contour along with it. The resultant picture is as shown in Fig. 15(c). The impact on the discontinuity equation (2.3) is that ω_1 must be integrated along a path[13,14] that loops around its threshold ω_t as is indicated in Fig. 15(d).

In the case of Fig. 15(b), for which s is in B_1, ω_1 is integrated over the physical region from x to y. In fact, as σ' is reduced to the threshold σ_t, x and y approach each other, corresponding to the fact that the two-particle phase space of the σ' channel vanishes and the normal threshold is reached. In the case of Fig. 15(d), however, the integration between x and y has an extra anomalous piece. Equation (2.3) should then be written as

$$M_\sigma(s\pm, \sigma'+, \omega)$$

$$= h(s\pm, \sigma'+)\left[\int_x^y d\omega_1 A(\sigma'-, \omega_2) M(s\pm, \sigma'+, \omega_1\pm) \right.$$

$$\left. + \int_0^x d\omega_1 A(\sigma'-, \omega_2) M_{\omega_1}(s\pm, \sigma'+, \omega_1\pm) \right], \quad (3.4)$$

where M_{ω_1} is the discontinuity of $M(s,\sigma',\omega_1)$ across the two-particle unitarity cut in the ω_1 channel, defined in a way analogous to (2.3). Evidently, the complex part of the contour integration in Fig. 12 is eliminated at the expense of complicating the discontinuity equation.

As $s+$ approaches $[(\sigma'+)^{1/2} + m_3]^2$, the branch point β' pushes the contour of integration in the z plane to $-\infty$. Thus, a singularity occurs at $s = [(\sigma'+)^{1/2} + m_3]^2$; this is a singularity of the second type.[10] If we fix the branch cut along its natural position, then this singularity can be reached only by continuation across the cut, and is therefore not on the principal sheet.

If the amplitude $A(\sigma,\omega_2)$ in (3.3) is not regarded as a constant but has, in fact, a two-particle unitarity cut in the σ channel, one may question whether the integrand $A(\sigma-)M(\sigma+)$ can be written equivalently as $A(\sigma+)M(\sigma-)$. To show that they are equivalent, we use the convention $S(\sigma-)S(\sigma+) = 1$ and find that, in the abbreviated notation where phase-space integrations over products of amplitudes are implied,

$$F(\sigma-) \equiv A(\sigma+)M(\sigma-) - A(\sigma-)M(\sigma+)$$

$$= [A(\sigma+) - A(\sigma-)]M(\sigma-) - A(\sigma-)$$

$$\times [M(\sigma+) - M(\sigma-)] = A(\sigma-)F(\sigma-).$$

This being an integral equation with an $\mathcal{L}^2$ kernel except at the poles of $A(\sigma)$, $F(\sigma)$ vanishes everywhere except

[13] V. V. Anisovich, A. A. Ansel'm, and V. N. Gribov, Zh. Eksperim. i Teor. Fiz. **42**, 224 (1962) [English transl.: Soviet Phys.—JETP **15**, 159 (1962)].
[14] C. Kacser, Phys. Rev. **132**, 2712 (1963).

at certain isolated points; analyticity then requires that it be identically zero.

Finally, we make some remarks regarding the situation where ω_t is greater than $(m_3+m_7)^2$. In this case x_3 is less than -1, so the solution $x_2{}^{\pm}$ is a hyperbola, shown in Fig. 5(b). The associated singularities $s_{\pm}{}''(\sigma')$ in the s plane are real if $\sigma'>\sigma_t$. The natural branch cut joining $s_{\pm}{}''(\sigma')$ is as shown in Fig. 16(a). The value of β'' at which the cut turns complex can be determined by solving (2.10) for $E_3(s,\sigma')$, which gives

$$E_3(s,\sigma')=\frac{-E_7M^2\pm p_7\beta''[M^4-4m_3{}^2(E_7{}^2-p_7{}^2\beta''^2)]^{1/2}}{2(E_7{}^2-p_7{}^2\beta''^2)},$$

where $M^2=\omega_t-m_3{}^2-m_7{}^2$. Defining β_0 to be the positive value of β'' for which the square root is zero, i.e.,

$$\beta_0(\sigma')=+[1-(M^4-4m_3{}^2m_7{}^2/4m_3{}^2p_7{}^2)]^{1/2},$$

we see that for real $\sigma'>\sigma_t$ and a sufficiently small positive value of $\omega_t-(m_3+m_7)^2$, β_0 is in the interval $(0,1)$; clearly, $E_3(s,\sigma')$ (and therefore s itself) is complex if $-\beta_0<\beta''<\beta_0$, but is real if $\beta_0\leqslant|\beta''|\leqslant 1$. Similar behavior can be found for the branch cut in the σ' plane. A sketch of it is shown in Fig. 16(b). It is interesting to note that when x_2 is reduced to a value less than $-x_3$ but greater than $+1$, i.e.,

$$(m_6+\omega_t{}^{1/2})^2<s<\omega_t+m_6[m_6+m_7+(\omega_t-m_3{}^2)/m_7],$$

the singularity $\sigma_-{}''(s)$ moves to the left, goes counterclockwise around the threshold σ_t, and then retreats to the right again, staying just below the real axis. At this point this singularity of M_σ can produce a pinch singularity for the $M(s,\sigma)$ amplitude in the *physical* region.[15] The branch cut attached to it is in the unphysical sheet, as is required by the homotopy condition.

IV. DISCONTINUITY EQUATIONS FOR THE THREE-PARTICLE CHANNEL

In this section we want to derive the discontinuity across the three-particle unitarity cut in the s channel. The two-particle σ-channel discontinuity equation in the principal sheet is given by (3.3), which we rewrite here in terms of angular integration as

$$M_\sigma(s\pm, \sigma+, \omega)$$
$$=\rho(\sigma+)\int d\Omega_\sigma A(\sigma-, \omega_2)M(s\pm, \sigma+,\omega_1\pm). \quad (4.1)$$

This equation has the following two properties:

(a) In the physical regions the M function in the integrand is evaluated above (or below) the ω_1 unitarity cut according as s is above (or below) its unitarity cut, independent of which side of the real axis ω is on.

(b) $M_\sigma(s,\sigma,\omega)$ can have no singularities in the physical region of the ω variable when s and σ are physical.

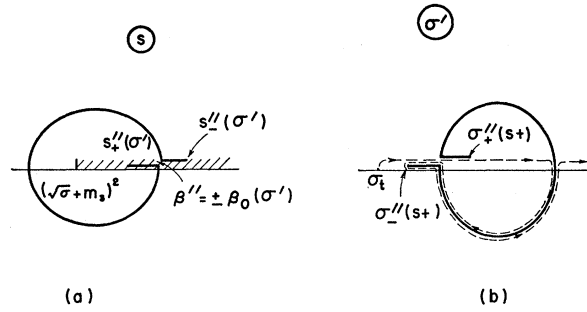[15] P. V. Landshoff, Phys. Letters **3**, 116 (1962).

FIG. 16. Natural positions of the branch cuts of M_σ in s and σ' planes for $\omega_t>(m_3+m_7)^2$.

The first property above has already been established by the analysis made in the last section. We now give arguments to establish the second. Referring to Fig. 1(b), let us consider the three-momentum vectors of particles 3, 4, and 7 in the rest frame of the σ channel. Denote the angles between 3 and 4 by ψ, between 3 and 7 by θ, and between 4 and 7 by χ. Clearly, the variables ω, ω_1, and ω_2 depend on the angles ψ, θ, and χ, respectively. If the polar axis is placed along the direction of vector 7, then ψ can be expressed in terms of θ, χ and the azimuthal angle $\phi_\theta-\phi_\chi$. In (4.1), the angles of integration can be either θ, ϕ_θ, or χ, ϕ_χ. Now, the integral can have a singularity in the ω variable only if both $A(\sigma,\omega_2)$ and $M(s,\sigma,\omega_1)$ in the integrand contribute terms that depend on the angle of integration; otherwise, the integrand can be made independent of ψ and the integral is then no longer a function ω. Since ω_2 is a momentum transfer variable of a four-line amplitude, singularities of $A(\sigma, \omega_2)$ in the ω_2 channel are always located at unphysical angles of χ, whereas $M(s,\sigma,\omega_1)$ can have singularities at physical values of θ. These singularities must pinch the contour of integration in order to yield a singularity of $M_\sigma(s,\sigma,\omega)$ in the ω variable. It is clear from the angular relationship between ψ, θ, and χ that it is impossible to obtain physical values of ψ from a combination of θ and χ where χ is unphysical. Hence, we find that in general $M_\sigma(s,\sigma,\omega)$ does not have discontinuities at physical values of ω, i.e., $M_\sigma(s,\sigma,\omega+)=M_\sigma(s,\sigma,\omega-)$ for ω physical. This is true for σ in both sections of region B (see Fig. 12).

On the basis of properties (a) and (b), the derivation of the discontinuity equation in the s variable in the physical region of a three-particle state is extremely simple. To specify the subenergies of the M function more completely, we need also the variable ν, defined to be $(k_3+k_5)^2$. Although it satisfies the constraint

$$\nu=\sum_{i=1}^{3} m_i{}^2+s-\sigma-\omega,$$

we must independently specify whether it is above or below its own unitarity cut. Thus, in abbreviated nota-

tion, we have

$$M(s+, \sigma+, \omega+, \nu+) - M(s+, \sigma-, \omega+, \nu+)$$
$$= A(\sigma-)M(s+, \sigma+, \omega'+, \nu'+),$$
$$M(s+, \sigma-, \omega+, \nu+) - M(s+, \sigma-, \omega-, \nu+)$$
$$= A(\omega-)M(s+, \sigma'+, \omega+, \nu'+),$$
$$M(s+, \sigma-, \omega-, \nu+) - M(s+, \sigma-, \omega-, \nu-)$$
$$= A(\nu-)M(s+, \sigma'+, \omega'+, \nu+).$$

Adding the expressions yields

$$M(s+, \sigma_i+) - M(s+, \sigma_i-)$$
$$= T_D(\sigma_i-)M(s+, \sigma_i+), \quad (4.2)$$

where σ_i designates σ, ω, and ν collectively, and T_D is the sum of the disconnected parts of the three-particle amplitude. The over-all discontinuity equation (1.1) derived by Stapp[3] on general grounds without using unitarity or Hermitian analyticity states that

$$M(s+, \sigma_i+) - M(s-, \sigma_i-)$$
$$= T(s-, \sigma_i-, \sigma_i'-)M(s+, \sigma_i'+), \quad (4.3)$$

where $T(s, \sigma_i, \sigma_i')$ is the general three-in, three-out scattering amplitude. Subtracting (4.2) from (4.3), we have finally

$$M(s+, \sigma_i-) - M(s-, \sigma_i-)$$
$$= T_C(s-, \sigma_i-, \sigma_i'-)M(s+, \sigma_i'+), \quad (4.4)$$

where $T_C(s,\sigma_i,\sigma_i')$ represents the connected part of the three-particle scattering amplitude. In a similar way we can derive

$$M(s+, \sigma_i+) - M(s-, \sigma_i+)$$
$$= T_C(s+, \sigma_i+, \sigma_i'+)M(s-, \sigma_i'-). \quad (4.5)$$

Equations (4.4) and (4.5) are the discontinuity equations in the s variable across the three-particle unitarity cut with the subenergy variables kept fixed.

VI. CONCLUSION

Maximal analyticity is interpreted to mean that a representation of the M function on the physical sheet can be developed by starting with contributions from Cauchy contours associated with discontinuities across the various normal cuts (poles included), and then introducing these contributions iteratively into the formulas expressing the discontinuities. The physical sheet is bounded by the normal cuts together with additional cuts that emerge from these as one increases the effective external masses from zero. These additional cuts come from extra parts of the contours, which run along the cuts of the discontinuity functions. The cuts of the discontinuity functions are determined by defining the function everywhere (i.e., on its principal sheet) by means of the original integral formula, with fixed (undistorted) contours. The M functions are expressed to a certain "order" by using the *exact M* functions in the discontinuity formulas across the various cuts, but including contributions from only those cuts obtained by carrying the iteration scheme to a certain order.

The procedure has been applied to the case of a two-particle to three-particle production amplitude in certain lowest nontrivial orders. It has been verified that the physical sheet defined in this way contains the physical regions corresponding to various crossed reactions, and that the cuts do not prevent continuation between the physical regions. The knowledge of the analytic structure is then used to determine from original discontinuity formulas, which give the simultaneous discontinuities across all cuts, the simple formulas for the discontinuities across the individual cuts in the two-particle subenergies of the three-particle channel and across the cut in the total energy.

ACKNOWLEDGMENTS